Oxidation of Glycosphingolipids under Basic Conditions: Synthesis of Glycosyl "Serine Acids" as Opposed to "Ceramide Acids". Precursors for Neoglycoconjugates with Increased Ligand Binding Affinity†

M. Mylvaganam,‡ L.-J. Meng,§ and C. A. Lingwood*,‡,||

Division of Immunity, Infection, Injury and Repair, Research Institute, The Hospital for Sick Children, Toronto, Ontario M5G 1X8, Canada, Departments of Biochemistry and Laboratory Medicine & Pathobiology, University of Toronto, Toronto, Ontario, Canada, and Mass Spectrometry Laboratory of the Medical Research Council of Canada, University of Toronto, Toronto, Ontario, Canada

Received March 23, 1999; Revised Manuscript Received June 11, 1999

ABSTRACT: Two types of oxidative cleavage of the double bond of glycosphingolipids (GSLs) are described. Oxidation of peracetylated GSL precursors with stoichiometric proportions of $KMnO_4$ and an excess of $NaIO_4$, in a neutral aqueous *tert*-butanol solvent system, gave nearly quantitative yields of the glycosyl ceramide acid, 2-hydroxy-3-(*N*-acyl)-4-(*O*-glycosyl)oxybutyric acid [Mylvaganam, M., and Lingwood, C. A. (1999) *J. Biol. Chem*. *274*, 20725−20732]. However, if the reaction medium was made alkaline, the hydroxyallylic function of the sphingolipid, as a whole, was oxidized and the glycosyl serine acid, 2-(*N*-acyl)-3-(*O*-glycosyl)oxypropionic acid, was obtained in good yield. This represents a new type of oxidation reaction. Optimized conditions gave glycosyl ceramide or serine acids with greater than 90% selectivity and in good yields (90%). Oxidation of dGSLs gave serine and ceramide oligosaccharides, devoid of hydrocarbon chains. An intriguing glycosyl species containing 5-hydroxy-4-oxo-3-hydroxy-2-(*N*-acyl)sphingosine (hydroxy−acyl intermediate) was identified via ESMS analyses. We propose that further oxidation of this intermediate is pH-dependent and will be oxidized to either serine or ceramide acids. On the basis of MS−MS analysis of specific homologues of serine and ceramide acids, two types of collision-induced dissociation (CID) patterns have been established. These CID patterns were then used in the identification of serine and ceramide acids synthesized from natural GSL samples. Also, on a qualitative basis, this oxidation protocol, in conjunction with ESMS, provides a novel method for characterizing the aglycone composition (acyl chain length, unsaturation position, dihydrosphingosine content, etc.) of natural GSLs. A novel class of neohydrocarbon conjugates were synthesized by coupling the acids to rigid hydrocarbon frames such as 2-aminoadamantane. Preliminary studies with conjugates derived from globotriaosyl ceramide (Gb_3C), lactosyl ceramide (LC), and galactosyl ceramide (GalC) bound verotoxin with the expected specificity but with affinities much greater than that of the natural glycolipid. Also, the ceramide acid-based conjugates were better ligands than serine acid conjugates.

Among the repertoire of cell membrane components, glycosphingolipids (GSLs)[1] form a unique class of amphiphathic molecules (*1*−*3*). The glycone and aglycone components of glycolipids are concatenated by a "serine-like" moiety. Often, this serine-like unit is chemically modified during the investigation of glycolipid function. In this respect, versatile reactions were the hydrolysis of the acyl chain (*4*−*7*) and/or the oxidation of the sphingosine double bond (*8*−*10*). Furthermore, the oxidation of dGSLs will give the "oligosaccharide" component of natural GSLs, devoid of hydrocarbon chains. Such oligosaccharides contain the serine-like moiety attached to the reducing terminus, and, as illustrated in Scheme 1, could be conveniently used in the synthesis of neoglycoconjugates. Although similar oligosaccharides can be synthesized from hexose precursors, such endeavors require considerable time and (synthetic and organic) skill (*11*). Therefore, a facile oxidation protocol for the cleavage of the sphingosine double bond (of GSL and dGSL) should circumvent such a necessity (at least on a preliminary investigative level). Such a method should therefore provide a convenient route for transforming a naturally occurring GSL into various neoglycoconjugates (Scheme 1).

We recently elaborated on the oxidation of sphingolipids under neutral-pH conditions, i.e., the synthesis of glycosyl ceramide acids (*12*). Oxidation of peracetylated GSLs using limited amounts of $KMnO_4$ and an excess of $NaIO_4$ (*13*) in an aqueous *tert*-butyl alcohol solvent system gave good yields (>90%) of the desired acids. This protocol was successfully used in the synthesis of glycosyl ceramide acids from a variety of neutral (GalC, GlcC, LC, Gb_3C, Gg_3C,

† This work was supported by Canadian MRC Grant MT13073 and NIH Grant R01 DK52098.

* Corresponding author. Telephone: (416) 813-5998. Fax: (416) 813-5993. E-mail: cling@sickkids.on.ca.

‡ The Hospital for Sick Children.

§ Mass Spectrometry Laboratory of the Medical Research Council of Canada, University of Toronto.

|| Departments of Biochemistry and Laboratory Medicine & Pathobiology, University of Toronto.

10.1021/bi990669m CCC: $18.00
Published on Web 07/29/1999

Gb_4C, and Gb_5C) and charged (SGC and GM_1C) GSLs (*12*). The efficacy of the method was demonstrated by synthesizing BSA−ceramide acid conjugates and investigating their interactions with HIV coat protein gp120. These studies showed that glycoconjugates derived from galactosyl ceramide acids were better ligands than those derived from deacyl GalC where the latter was coupled via the amine. The ceramide acid or the deacyl GalC conjugates differ only in the organization of their aglycone, where the former has the acyl chain intact whereas the latter has the sphingosine intact. This suggests that aglycone organization (*4*, *14*), particularly the region adjacent to the reducing end of the glycone, plays a role in the presentation of glycone in protein−GSL recognition.

This report describes the synthesis of two types of acids, 2-hydroxy-3-(*N*-acyl)-4-(*O*-glycosyl)oxybutyric acid (glycosyl ceramide acid) or 2-(*N*-acyl)-3-(*O*-glycosyl)oxypropionic acid (glycosyl serine acid). The serine acids result from a previously undescribed oxidation condition in which the hydroxyl allyl (^{3}CHOH−^{4}CH=^{5}CH) group is oxidized to carboxylic acid (to ^{3}COOH). These oxidation protocols could be carried out with microgram quantities of peracetylated GSLs or dGSLs, and the desired products are formed with good selectivity (∼90%) and yield (∼90%). Preliminary binding studies with a novel class of unidentate hydrocarbon conjugates derived from glycosyl serine and ceramide acids are presented.

EXPERIMENTAL PROCEDURES

Materials. Solvents (DCM, ^{t}BuOH, ^{i}PrOH, DCE, Py, Et_2O, MeOH, and $CHCl_3$) were purchased from either Caledon (Georgetown, ON) or Aldrich (Milwaukee, WI), and EtOH was purchased from Commercial Alcohols Inc. (Brampton, ON). Reagents were purchased from the following suppliers: 0.5 N H_2SO_4 solution, acetic anhydride, and $AdaNH_2$ from Aldrich, ANALAR $KMnO_4$ and ANALAR $NaHSO_3$ from BDH (Toronto, ON), behenic acid ($C_{22}H_{44}O_2$), palmitic acid ($C_{16}H_{32}O_2$), stearic acid ($C_{18}H_{36}O_2$), erucic acid ($C_{22}H_{42}O_2$), oleic acid ($C_{18}H_{34}O_2$), Boc-NO, Et_3N, HODBT, and EDAC from Sigma (St. Louis, MO), and HOAT from Fluka (Oakville, ON). Chromatographic materials [Silica gel 60 (40−63 μm or 230−400 mesh) and aluminum-backed nanosilica plates (alugram NanoSIL GI UV_{254}, Macherey & Nagel)] were supplied by Caledon. Reverse phase C-18 cartridges were obtained from Waters (Mississauga, ON) and 4 Å molecular sieves from Fisher.

Glycolipids. LC, Gb_3C, and Gb_4C were purified from human kidney (*15*); Gb_5C was purified from sheep blood (*16*), and GM_1C was purified from bovine brain (*17*) according to previously published procedures. GalC, GlcC, and SGC were purchased from Sigma. Deacylated derivatives, Gb_3S, and GalS (phychosine) were prepared by saponification of Gb_3C and GalC at 102 °C with 1 M NaOH in MeOH for 3 h (*16*). All silica gel column chromatography was performed under gravity.

Synthesis of Gal^{B}C, Gal^{P}C, Gal^{S}C, Gal^{O}C, and Gal^{E}C. To a solution of GalS (2 mg, 4 μmol) in 5:1 CH_3CN/Et_3N (2 mL) were added fatty acid (2 mg, ∼2 equiv), HOAT (30

Scheme 1: Types of Glycoconjugates That Can Be Synthesized from Serine and Ceramide Acids[a]

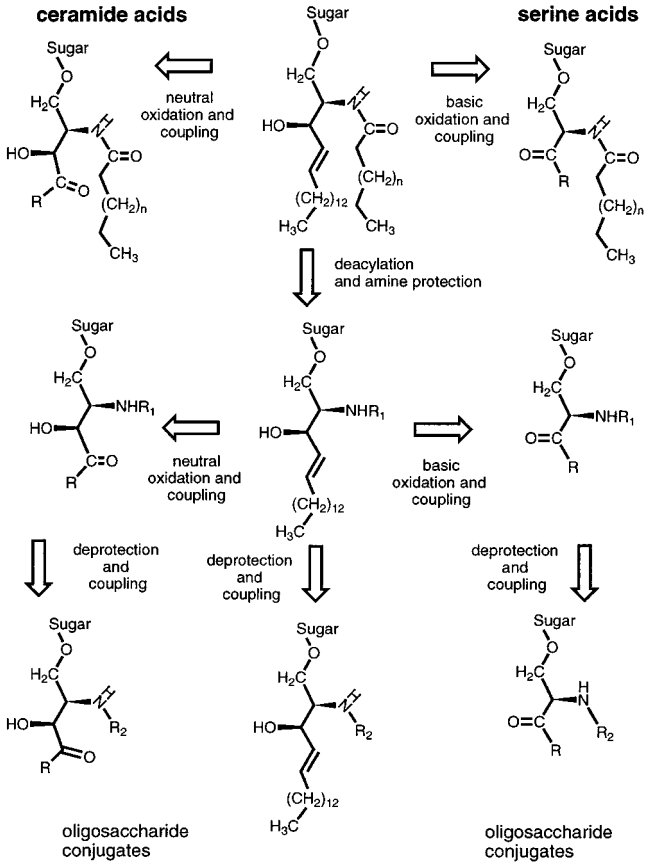

[a] Oxidized acids from dGSLs are devoid of hydrocarbon chains and enable coupling at two sites. R_1 is ^{t}Boc, CF_3CO, etc. R and R_2 are hydrocarbon frames such as adamantane, norbonane, peptides, proteins, etc. Sugar corresponds to various glycones of GSLs.

[1] Natural glycosphingolipids (GSLs) terminate with "C" (for ceramide), and deacyl or lyso GSLs (dGSLs) terminate with "S" (for sphingosine), for example, galactosyl ceramide (GalC) and lyso galactosyl ceramide (GalS). Other GSLs include glucosyl ceramide (GlcC), sulfogalactosyl ceramide (SGC), globotriaosyl ceramide (Gb_3C), globotetraosyl ceramide (Gb_4C), and monosialylganglioside (GM_1C). Acyl chains on ceramide were specified as follows. Gal^{B}C (Gal^{22}C), Gal^{P}C (Gal^{16}C), Gal^{S}C (Gal^{18}C), Gal^{O}C (Gal$^{18:1}$C), and Gal^{E}C (Gal$^{22:1}$C) refer to galactosyl ceramide homologues containing behenic (C-22), palmitic (C-16), stearic (C-18), oleic (C-18:Z9), and erucic (C-22:Z13) acyl chains. Dihydrosphingosine-containing GSLs are abbreviated as Gal*C. All abbreviations following the dot indicate modifications to the ceramide or the sphingosine, for example, galactosyl *N*-acetyl sphingosine (GalS·NAc), galactosyl *N*-*tert*-butoxycarbonyl sphingosine (GalS·N^{t}Boc), etc. Acids derived from the oxidation of GSLs and dGSLs are abbreviated as GSL·^{C}COOH, GSL·^{S}COOH, dGSL·^{C}COOH, or dGSL·^{S}COOH, for example GalC·^{C}COOH, GalC·^{S}COOH, GalS·N^{t}Boc^{C}COOH, etc. Superscripts "C" and "S" denote ceramide and serine acid, respectively. GSLs with unsaturated acyl chain, upon oxidation, yield dicarboxylic acids, denoted as, for example, GalC·^{C}COOH^{n}COOH, where *n* is the 1,*n*-dicarboxylic acyl chain. Neohydrocarbon glycoconjugates are denoted as, for example, Gb_3C·^{C}CONHAda, Gb_3C·^{S}CONHAda, etc. The standard numbering scheme is used; for example, a sphingosine double bond will be denoted as ^{3}CHOH−^{4}CH=^{5}CH−^{6}CH$_2$, and the moiety ^{3}CHOH−^{4}CH=^{5}CH is termed the hydroxyallylic group. Other abbreviations are as follows: VT, verotoxin; HK, human kidney; PH1, monoclonal anti-VT antibody; MS, mass spectra or mass spectroscopy; ESMS, electrospray mass spectroscopy; FAB, fast atom bombardment; PBS, phosphate-buffered saline; BSA, bovine serum albumin; TLC, thin-layer chromatography; H_2O^S, 0.88% KCl solution; DCM, dichloromethane; ^{t}BuOH, *tert*-butyl alcohol; ^{i}PrOH, isopropyl alcohol; DCE, 1,2-dichloroethane; Py, pyridine; Et_2O, diethyl ether; MeOH, methanol; EtOH, ethanol; $AdaNH_2$, 2-aminoadamantane; Boc-NO, *N*-*tert*-butoxycarbonyloxyimino-2-phenylacetonitrile; Et_3N, triethylamine; HODBT, 3-hydroxy-1,2,3-benzotriazin-4(3*H*)-one; EDAC, 1-ethyl-3-[3-(dimethylamino)propyl]carbodiimide; HOAT, 1-hydroxy-7-azabenzotriazole.

μL of a 0.2 M solution in 5:1 CH_3CN/Et_3N, 6 μmol), and solid EDAC (2−3 mg, 10−15 μmol), and the mixture was stirred at 50 °C for 4 h and monitored by TLC (80:20:2 $CHCl_3/MeOH/H_2O^S$). Upon completion, the reaction mixture was dried under a stream of N_2 and the crude product was dissolved in DCM (1 mL) and loaded onto a silica column (0.5 cm × 10 cm silica gel in 98:2 $CHCl_3$/MeOH). Excess fatty acid was eluted with 85:15 DCE/^{i}PrOH (20 mL), and the product was eluted with 80:20:2 $CHCl_3/MeOH/H_2O$ (six 4 mL fractions were collected). The estimated yield as determined by TLC was >90%.

Synthesis of GalS·N^{t}Boc. To a solution of GalS (1 mg, 1−2 μmol) in methanol (1 mL) was added solid Boc-NO (1 mg, 4 μmol), and the mixture was stirred at 60 °C for 2 h. Methanol was removed under a stream of nitrogen, and the residue was dissolved in 98:2 $CHCl_3$/MEOH (1 mL) and loaded onto a silica column (0.5 cm × 5 cm silica gel in 98:2 $CHCl_3$/MeOH). The product was eluted with 90:15:1 $CHCl_3/MeOH/H_2O$. The estimated yield as determined by TLC was >90%.

Synthesis of Peracetylated Derivatives. A 1:2 mixture of acetic anhydride and pyridine was added to a dried sample of GSL or dGSL (to a final concentration of 1 mg/mL) and stirred at 37 °C for 2 h. The reactions were monitored by TLC (80:15 DCE/^{i}PrOH), and upon completion, the mixture was dried under a stream of N_2. The crude material was dissolved in DCE (1 mL) and was loaded onto a silica column (for 3 mg of crude, 0.5 cm × 5 cm silica gel in DCE) and eluted with 25 mL of *Y* DCM/MeOH, where *Y* was varied from 100 μL, in increments of 100 μL (for each solvent composition, six 4 mL fractions were collected). The mobilities of peracetylated derivatives during column chromatography vary significantly with small changes in the activity of the silica gel. Concomitant changes to the polarity of the eluent may be necessary. The purity (important for the oxidation to proceed smoothly) of the product was checked by TLC, where the plates were developed with I_2 vapor.

Oxidation Reactions. The reagents were a 2:1 mixture of ^{t}BuOH and H_2O and solutions of $NaIO_4$ (0.4 M), K_2CO_3 (0.25 M), and $KMnO_4$ (0.05 M). The quenching solution was a 5:1 mixture of a 0.25 M $NaHSO_3$ solution and 0.5 N H_2SO_4.

Peracetylated glycolipid [$GSL(OAc)_n$, 0.5 mg or $dGSL\text{-}(OAc)_n$, 0.3 mg, which corresponds to 1−0.3 μmol] was dissolved in aqueous ^{t}BuOH (500 μL), and solutions of $NaIO_4$ (30 μL, 10 μmol), K_2CO_3 (40 μL, 10 μmol), and $KMnO_4$ (15 μL, 0.75 μmol) were added in the given sequence. The resulting turbid purple mixture was stirred at room temperature and was monitored by TLC every 4 h. The TLC solvent system for monitoring the oxidation of $GSL(OAc)_n$ was 90:15:1 $CHCl_3/MeOH/H_2O^S$ and for $dGSL\text{-}(OAc)_n$ was 80:20:2 $CHCl_3/MeOH/H_2O^S$. When pure precursors were used, catalytic regeneration of $KMnO_4$ proceeded smoothly until the reaction was terminated. Otherwise, the purple colored reaction mixture diminished in intensity with concomitant formation of MnO_2. In such cases, additional aliquots (5 μL) of $KMnO_4$ solution were added. The reaction was quenched by the addition of 2 mL of quenching solution and 1 mL of water, and the resulting colorless solution was extracted with Et_2O (three times, 5 mL each). Occasionally (due to insufficient quenching), the ether extract turned yellow, and in such cases, the combined extracts were washed with 1 mL of quenching solution. The ether extract was washed (twice, 1 mL each) with water and dried under a stream of N_2 at 25 °C. Residual water in the product was removed by adding absolute EtOH (1−2 mL) and evaporating under a stream of N_2.

Modified Workup. A different workup procedure was employed for the isolation of serine and ceramide acids derived from the oxidation of charged GSLs [for example, from $(OAc)_4$SGC] and for most of the deacyl GSLs. In these cases, even though the alcoholic functions of these acids were peracetylated, they partitioned poorly into the Et_2O phase. In such cases, the reaction was quenched with an excess of solid $NaHSO_3$ (50 mg). The colorless (occasionally pale yellow) suspension was dried on a rotary evaporator and extracted (three times, 5−7 mL) with 80:20:2 $CHCl_3/MeOH/H_2O$, and the salts were removed by passing the combined extract through a silica column (0.5 cm × 4 cm silica gel in 80:20:2 $CHCl_3/MeOH/H_2O$) and then dried.

Synthesis of glycosyl ceramide acids was carried out using reaction conditions and the workup procedures that were almost identical to those for the synthesis of glycosyl serine acids, except K_2CO_3 was not employed in the reaction.

Glycosyl ceramide and serine acids obtained after the workup procedure will contain some unoxidized materials (approximately 5%, mainly dihydrosphingosine species; see Figure 1). Further purification of the glycosyl acids depends on the type of glycoconjugate that will be derived from them. For example, to synthesize neoglycoproteins (BSA conjugates), the purification of glycosyl acids from the unoxidized material is unnecessary. Crude material obtained after workup could be deprotected and coupled to the protein, and during the purification of neoglycoprotein, the unoxidized material will be removed along with reagents used for the coupling (*12*). Therefore, appropriate methods of purification are described within the context of glycoconjugate synthesis.

Deprotection of the glycosyl serine and ceramide acids was carried out by treating dried material (0.5 mg) with a triethylamine solution (1 mL of 2:6:10 $Et_3N/MeOH/H_2O$) at 37 °C overnight. The mixture was then dried under a stream of N_2 and the residue redissolved in ethanol.

Synthesis of Neohydrocarbon Conjugates. Oxidized material (0.5 mg) obtained after workup was dissolved in DCE (0.5 mL) and loaded onto a silica column (0.5 cm × 3 cm silica gel in DCE) and eluted with 25 mL of *Y* DCM/MeOH, where *Y* was varied from 100 μL, in increments of 100 μL (for each solvent composition, six 4 mL fractions were collected). This step elution chromatography will remove the unoxidized dihydrosphingosine-containing species. The peracetylated glycosyl serine or the ceramide acids were then eluted with methanol (3−5 mL) and dried under a stream of N_2. To a solution (in 5:1 CH_3CN/Et_3N, 1 mg/mL) of peracetylated glycosyl ceramide or serine acid were added the following reagents in the given order: $AdaNH_2$ (1:1 by weight), HODBT (1:1 by weight), and solid EDAC (1 mg). The reaction was monitored by TLC (90:15:1 $CHCl_3/MeOH/H_2O^S$) for 6 h. The coupled products migrate closer to solvent front. Upon completion, the reaction products were dried under a stream of N_2, dissolved in DCE, and purified on a mini silica column (for a 0.5 mg scale preparation, 0.5 cm × 2 cm silica gel column), as described above (using a 25 mL *Y* DCM/MeOH solvent system). Peracetylated neohy-

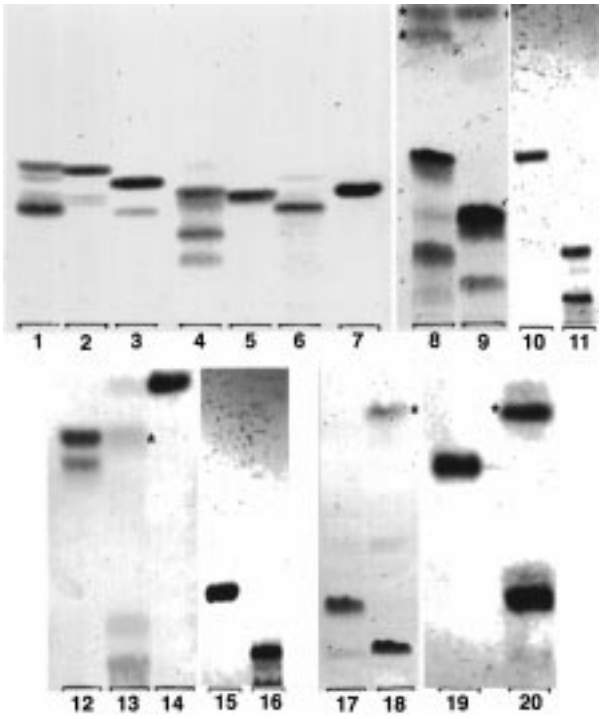

FIGURE 1: TLCs (nanosil plates, visualized with orcinol) showing the relative migration of serine and ceramide acids: lane 1, $(OAc)_4GalC\cdot^{S}COOH$; lane 2, $(OAc)_4Gal^{B}C\cdot^{S}COOH$; lane 3, $(OAc)_4Gal^{P}C\cdot^{S}COOH$; lane 4, $(OAc)_5GalC\cdot^{C}COOH$; lane 5, $(OAc)_5Gal^{B}C\cdot^{C}COOH$; lane 6, $(OAc)_5Gal^{P}C\cdot^{C}COOH$; lane 7, $(OAc)_5GalC$; lane 8, $(OAc)_9Gb_3C\cdot^{S}COOH$; lane 9, $(OAc)_{10}Gb_3C\cdot^{C}COOH$; lane 10, Gb_5C; lane 11, $Gb_5C\cdot^{S}COOH$; lane 12, SGG (upper) and SGC (lower); lane 13, $(OAc)_4SGC\cdot^{C}COOH$; lane 14, $(OAc)_4SGC$; lane 15, GM_1C; lane 16, $GM_1C\cdot^{S}COOH$; lane 17, $(OAc)_4GalS\cdot N^{t}Boc^{S}COOH$; lane 18, $(OAc)_5GalS\cdot N^{t}Boc^{C}COOH$; lane 19, Gb_3S; and lane 20, $Gb_3S\cdot NAc^{C}COOH$. Lanes 2 and 3, 5 and 6, and 17 and 18 show the products obtained from the oxidation of single homologues. In lanes 2 and 3, the minor bands correspond to bands in lanes 5 and 6, respectively. Multiple bands seen in other lanes (for example, in lanes 1, 4, 8, etc.) are a result of aglycone heterogeneity (*12*). Asterisks denote starting material and/or intermediates and/or GSLs with dihydrosphingosine. The following solvent systems were used: lanes 1−9, 17, and 18, 80:20:2 $CHCl_3$/MeOH/H_2O[S]; lanes 10−12, 60:40:9 $CHCl_3$/MeOH/H_2O[S]; and lanes 13−16, 19, and 20, 5:5:5:2:2 $CHCl_3$/MeOH/acetone/acetic acid/H_2O.

drocarbon conjugates were then deprotected with an Et_3N/MeOH/H_2O system (as described in the oxidation procedure).

Verotoxin Binding. A methanolic solution of natural GSL or the adamantyl conjugate was added to a 96-well microtiter plate and allowed to evaporate overnight. The wells were blocked with 0.2% BSA in PBS (BSA/PBS) for 1 h at room temperature. The wells were washed once with BSA/PBS, and 50 μL of VT_1 (verotoxin, 20 ng) in BSA/PBS was added to each well. The plate was incubated at room temperature for 2 h, washed three times with BSA/PBS, and incubated with 50 μL of PH1 (monoclonal anti-VT_1 antibody, 50 ng per well) (*18*) in BSA/PBS for 1 h. Bound antibody was detected after further washing with BSA/PBS and using an immunoperoxidase system and ELISA reader (*18*). Verotoxin TLC overlay assays were performed as previously described (*19*).

Mass Spectroscopy. This is the method of choice for microscale structural determination of natural GSL derivatives. All samples were dissolved in aqueous methanol (9:1 MeOH/H_2O) containing 0.1% NaCl to give a final concentration of 1 mg/mL. Electrospray mass spectra were acquired on an API III Plus triple-quadrupole mass spectrometer (PE Sciex, Thornhill, ON) fitted with an articulated pneumatically assisted nebulization probe. The spectrometer was operated at unit resolution (50% valley definition) over the mass range of *m*/*z* 50−2400. Samples were introduced into the electrospray ionization source at a flow rate of 10−20 μL/min using a LC pump. The electrospray needle was operated at 4.8 kV; the orifice voltage was set at 65 V, and nitrogen was used as the nebulization gas. Full scan mass spectra were acquired over the mass range of *m*/*z* 200−1500 by scanning the third mass spectrometer, Q3, using a *m*/*z* 0.2 step size and a 1 ms dwell time.

Scheme 2: Steps Involved in the Conversion of Natural GSLs to Serine and Ceramide Acids[a]

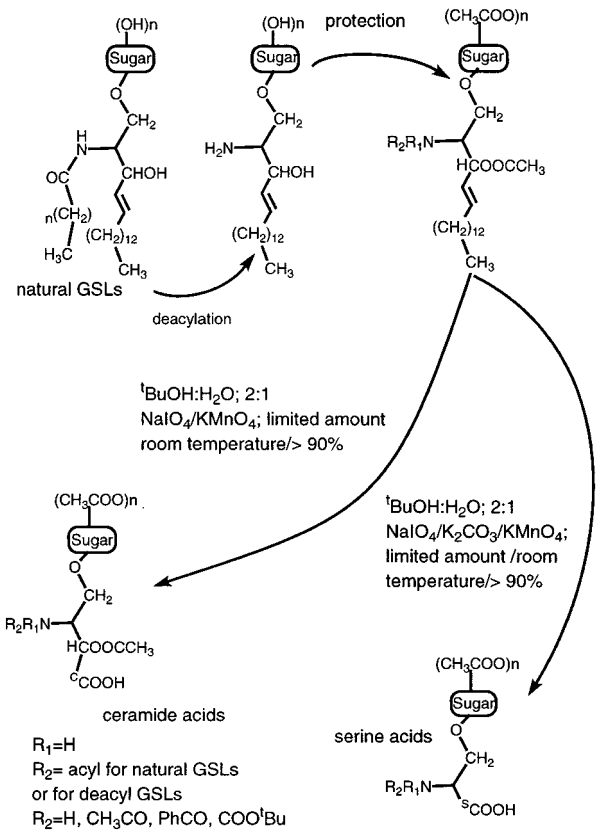

[a] When substituents R_1 and R_2 are small, the acids are termed serine and ceramide oligosaccharides. The notation $(OH)_n$ refers to all the hydroxyl groups on the glycone.

RESULTS AND DISCUSSION

The chemical steps involved in the synthesis of glycosyl serine and ceramide acids from natural and dGSLs are shown in Scheme 2. These acids, as depicted in Scheme 1, are useful precursors in the synthesis of various glycoconjugates. The oxidation step shown in Scheme 2 uses "off the shelf" reagents such as $NaIO_4$ and $KMnO_4$ [as opposed to ozonolysis (*9*)] and can be applied to microgram quantities of GSLs. The typical procedure involves the treatment of peracetylated GSLs or dGSLs with $KMnO_4/NaIO_4$ or $KMnO_4/NaIO_4/K_2CO_3$ catalytic systems in an aqueous ^{t}BuOH solvent system. Earlier investigations using $KMnO_4$ as an oxidant, $KMnO_4$/acetone (*10*) and $KMnO_4$/crown ether/benzene (*8*) systems, gave low yields of the desired products. In these cases, the heterogeneous nature of the reaction medium could

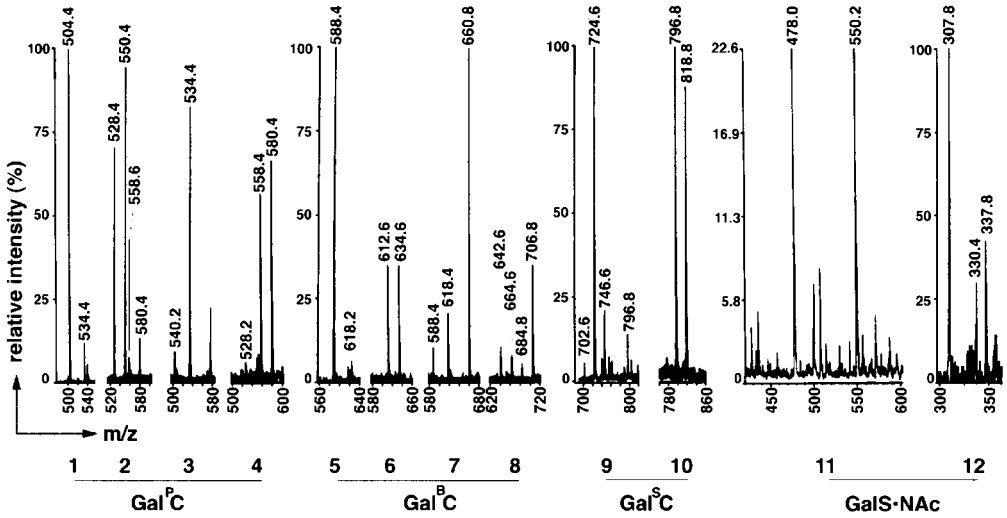

FIGURE 2: Parent ions seen in the ESMS of serine and ceramide acids derived from Gal^{P}C, Gal^{B}C, Gal^{S}C, and GalS·NAc. Spectra (300−1000 mass unit scan range) of samples 1−10 exhibited the depicted ions as the major ion species: spectrum 1, Gal^{P}C·^{S}COOH (negative mode); spectrum 2, Gal^{P}C·^{S}COOH (positive mode); spectrum 3, Gal^{P}C·^{C}COOH (negative mode); spectrum 4, Gal^{P}C·^{C}COOH (positive mode); spectrum 5, Gal^{B}C·^{S}COOH (negative mode); spectrum 6, Gal^{B}C·^{S}COOH (positive mode); spectrum 7, Gal^{B}C·^{C}COOH (negative mode); spectrum 8, Gal^{B}C·^{C}COOH (positive mode); spectrum 9, $(OAc)_4$Gal^{S}C·^{S}COOH (positive mode); spectrum 10, $(OAc)_5$Gal^{S}C·^{C}COOH (positive mode); spectrum 11, $(OAc)_5$GalS·NAc oxidized at an intermediate pH (positive mode); and spectrum 12, same sample used for spectrum 11, but deprotected with $Et_3N/MeOH/H_2O$ (negative mode). Relative intensity ratios (see Table 1) of parent ions, i.e., the serine:ceramide (or vice versa) ratios, are comparable to the ratios observed by TLC analysis (Figure 1). Samples 11 and 12 are from the oxidation of GalS·NAc using an intermediate pH, where serine and ceramide acids are formed in similar proportions. In samples 7 and 8, main peaks correspond to the monoacetylated (OAc)Gal^{B}C·^{C}COOH (from incomplete deprotection) species, which constitutes less than 5% of the sample. Apparently having just one hydroxyl group acetylated enhances the stability of the parent ion by approximately 100-fold.

Table 1: Parent Ions from the ESMS Spectrum Shown in Figure 2

precursor	neutral oxidation (adduct, %)	basic oxidation (adduct, %)
Gal^{P}C	558.4 (M^C + Na, 56)	528.4 (M^S + Na, 71)
	580.4 (M^C − H + 2Na, 47)	550.4 (M^S − H + 2Na, 95)
	534.4 (M^C − H, 83)	504.4 (M^S − H, 100)
	528.2 (M^S + Na, 6)[a]	558.6 (M^C + Na, 9)[a]
	504.2 (M^S − H, 9)[a]	580.4 (M^C + Na, 13)[a]
	(M^C = Gal^{P}C·^{C}COOH)	534.4 (M^C − H, 12)[a]
		(M^S = Gal^{P}C·^{S}COOH)
Gal^{BC}	642.6 (M^C + Na, 11)	612.6 (M^S + Na, 34)
	664.6 (M^C − H + 2Na, 8)	634.6 (M^S − H + 2Na, 34)
	684.8 (M^C + Na + Ac, 5)	588.4 (M^S − H, 100)
	706.8 (M^C − H + 2Na + Ac, 40)	618.2 (M^C − H, 3)[a]
	660.8 (M^C + Ac − H, 100)	(M^S = Gal^{B}C·^{S}COOH)
	618.4 (M^C − H, 21)	
	588.4 (M^S − H, 10)[a]	
	(M^C = Gal^{B}C·^{C}COOH)	
Gal^{SC}	796.8 (M^C + Na, 100)	702.6 (M^S + H, 6)
	818.8 (M^C − H + 2Na, 89)	724.6 (M^S + Na, 100)
	[M^C = Gal^{S}C$(OAc)_5$·^{C}COOH]	746.6 (M^S − H + 2Na, 22)
		796.8 (M^C + Na, 15)[a]
		[M^C = Gal^{S}C$(OAc)_4$·^{S}COOH]
GalS·NAc	478.0 (M^S + H, 23)	307.8 (M^S − H, 100)
	550.2 (M^C + H, 23)	337.8 (M^C − H, 48)
	[M^C = $(OAc)_5$GalS·NAc·^{C}COOH]	(M^C = GalS·NAc·^{C}COOH)
	[M^S = $(OAc)_4$GalS·NAc·^{S}COOH]	(M^S = GalS·NAc·^{S}COOH)

[a] Minor species, where the ratios of major to minor are inverted upon changing from neutral to basic conditions or visa versa.

have been an adverse factor (*12*). Use of the $KMnO_4/NaIO_4$ (*13*) catalytic system enabled us to maintain a homogeneous reaction medium. The $^{t}BuOH/H_2O$ solvent dissolves most of the ionic oxidants and hydrophobic peracetylated GSLs. The purity of the peracetylated glycosphingolipids (see Experimental Procedures) was important for the catalytic regeneration of $KMnO_4$. The protocol was designed such that it could accommodate up to a 50% variation in the concentrations of GSL precursors and therefore can be directly employed for similar quantities of different GSLs. Although in principle catalytic amounts of $KMnO_4$ should have been adequate, using closer to 1 equiv, i.e., in comparison to GSL precursor, decreased the reaction time significantly.

Oxidation under Basic Conditions. When K_2CO_3 was added to the mixture where oxidation was catalyzed by $KMnO_4/NaIO_4$, TLC analyses of the products showed the formation of a second product. Consistently (i.e., for different GSLs), the mobilities of these products on TLC were higher (higher R_f) than those of the products obtained under neutral conditions. A systematic study of this reaction was hampered due to the variations in the acyl chain of natural GSLs. TLC

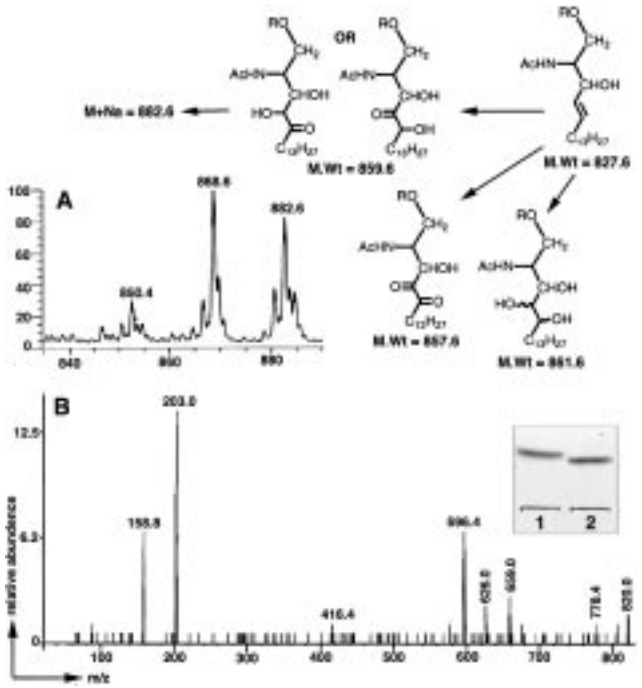

FIGURE 3: MS analyses of the intermediates. (A) FAB-MS (positive mode) of the deprotected intermediate isolated from the neutral oxidation of Gb_3S·NAc. Also shown are the possible diketone and dihydroxy intermediates, but the MS data are consistent only with the hydroxy acyl species (R being Gal1−4Gal1−4-Glc). (B) MS−MS spectrum of the 839 parent ion of the deprotected hydroxy acyl intermediate isolated from the neutral oxidation of Gal^BC (see Scheme 3). The TLC inset shows Gal^BC (lane 2) and the deprotected intermediate.

Scheme 3: Putative Fragmentation Analysis of the Deprotected Intermediate[a]

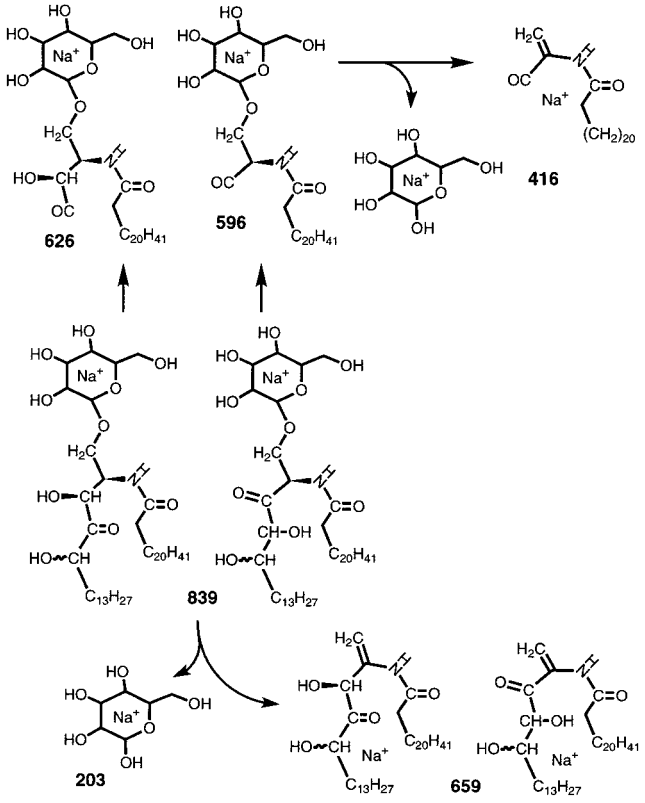

[a] The intermediate isolated from a neutral oxidation of Gal^BC was treated with Et_3N/MeOH/H_2O and then analyzed by ESMS (see Figure 3).

analyses of oxidized products from natural GSLs gave multiple bands, attributed in part to the different lengths of fatty acids, and to the dicarboxylic acids resulting from the oxidation of unsaturated fatty acids (*12*). Therefore, GalC homologues with single fatty acids were synthesized and oxidized under basic and neutral conditions. Optimizing the conditions gave the acids corresponding to the higher R_f band in an approximately 10:1 ratio where the R_f values of the minor products (i.e., lower band) were identical to that of glycosyl ceramide acid (Figure 1).

Mass spectra of the acids derived from Gal^BC, Gal^PC, Gal^SC, and GalS·NAc are shown in Figure 2, and peak assignments are listed in Table 1. Spectra 1−8 (in Figure 2) were obtained from samples that were treated with Et_3N/MeOH/H_2O (i.e., deprotected). Irrespective of the fatty acids on GalC, samples from basic oxidation gave parent molecular ions that were 30 mass units lower than those samples from neutral oxidation (compare spectra 1 and 2 with 3 and 4, and 5 and 6 with 7 and 8, in Figure 2). However, samples from basic oxidation that were not deprotected with Et_3N/MeOH/H_2O gave parent molecular ions that were 72 mass units smaller than those from neutral oxidation (compare spectra 9 with 10). Spectra 11 and 12 were from a dGSL precursor, GalS·NAc, where the oxidation was carried out at an intermediate pH (using only $^1/_{10}$ of K_2CO_3). Under these conditions, both products were formed in comparable proportions, and they differed by 72 mass units in the protected form and by 30 mass units in the deprotected form.

The above analyses suggest that one of the acetate functions is hydrolyzed during basic oxidation. However, treatment of $GalC(OAc)_5$ with $K_2CO_3/NaIO_4$ in ^{t}BuOH/H_2O or of the product from a neutral oxidation, $GlcC(OAc)_5$·^{C}COOH, with $K_2CO_3/KMnO_4/NaIO_4$ in ^{t}BuOH/H_2O showed no effect (TLC in Scheme 4). This shows that the acetate groups of neither the peracetylated precursors [$GSL(OAc)_n$] nor the peracetylated glycosyl ceramide acids [$GSL(OAc)_n$·^{C}COOH] were susceptible to hydrolysis under basic oxidation conditions; i.e., the ceramide acids cannot be converted into serine acids by treatment with $K_2CO_3/KMnO_4/NaIO_4$ in ^{t}BuOH/H_2O. On the basis of this observation, we hypothesize that a common intermediate **B** (see Scheme 4 and the following discussion) is formed during the oxidation. Depending on the pH of the reaction medium, intermediate **B** will be further oxidized to ceramide or serine acids. MS evidence so far strongly suggests that under basic conditions the hydroxy allylic group, ^{3}CH(OH)−^{4}CH═^{5}CH, of sphingosine is oxidized to ^{3}COOH (serine acid), whereas neutral conditions give the expected ^{3}CH(OH)−^{4}COOH (ceramide acid). Therefore, deprotected glycosyl serine and ceramide acids of a given GSL will differ by 30 mass units, whereas the same pair of acids in the peracetylated form will differ by 72 mass units.

*Hydroxy−Acyl Intermediate **B***. TLC analysis of an incomplete oxidation shows three major species which correspond to product, intermediate, and starting material (*12*). A FAB-MS profile of the deprotected intermediate isolated from a neutral oxidation of a deacyl GSL, Gb_3S·NAc, is depicted in Figure 3A. Of the three possible intermediates, dihydroxy, diketone, and hydroxy acyl (or hydroxy ketone), only the ion corresponding to the hydroxy acyl species was observed (*13*). The parent ion (M + Na, *m*/*e* 882) and

Scheme 4: Proposed Mechanism of Oxidation[a]

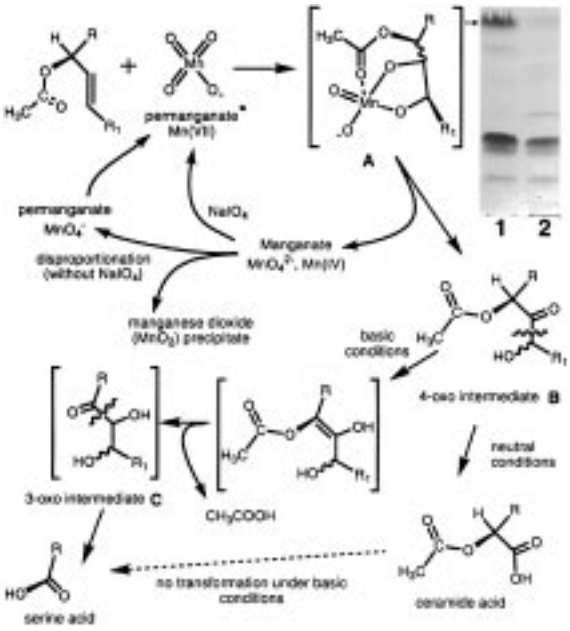

[a] R is the glycosyl group and R_1 $C_{13}H_{27}$. Intermediate **A** shows how the neighboring acetate group may play a role in the selective formation of **B** (termed in the text ^{3}COAc−^{4}CO−^{5}CHOH). The top right insert depicts the TLC analyses, which suggest that the ceramide acid cannot be oxidized to serine acid under basic conditions: lane 1, Glc(OAc)$_5$C·^{C}COOH; and lane 2, same sample from lane 1 treated with $KMnO_4$/$NaIO_4$/K_2CO_3 for 6 h (lane 2). The fastest species in lane 1 (indicated with an arrow) corresponds to intermediate **B** or **C** but not **A** and/or unreacted starting material.

probably peaks from successive loss of CH_2 (*m*/*e* 868) and water (*m*/*e* 850) are depicted in Figure 3A. Similarly, the deprotected intermediate isolated from the neutral oxidation of a natural GSL homologue Gal^{B}C also gave the expected molecular ions for the hydroxy acyl species (839, M + Na, 80%; and 817, M + H, 30%). For the Gal^{B}C case, the MS−MS spectrum of one of the parent ions (839, M + Na) is shown in Figure 3B and the analysis in Scheme 3. MS−MS analysis shows that the most favored modes of collision-induced dissociations (CIDs) were the loss of hexose and/or the cleavage between the carbonyl carbon and the adjacent CHOH unit (i.e., the CO−CHOH bond). This second mode of CID is useful in locating the position of the carbonyl group. Such CID has also been observed during the MS analysis of SGC containing α-hydroxylated fatty acids (*20*).

In Figure 3B, fragment ions at *m*/*e* 626 and 596 probably arise from two isobaric molecular ions containing ^{3}CHOH−^{4}CO−^{5}CHOH (4-oxo species) and ^{3}CO−^{4}CHOH−^{5}CHOH (3-oxo species) groups, respectively (Scheme 3). It was significant that there was no evidence for the presence of a 5-oxo species. It is important to note that the intermediates for which the MS spectrum is shown in Figure 3B were isolated from a neutral oxidation and were recorded after treating the sample with Et_3N/MeOH/H_2O. Therefore, even though the MS−MS spectrum shown in Figure 3B strongly suggests the presence of a 3-oxo intermediate, ^{3}CO−^{4}CHOH−^{5}CHOH, it is very unlikely that this was present in the sample prior to the treatment with Et_3N/MeOH/H_2O. Such a 3-oxo intermediate, even under neutral conditions, would have readily undergone oxidative cleavage between C3 and C4 to yield the serine acid (which was not found). However, the 4-oxo intermediate, ^{3}CHOH−^{4}CO−^{5}CHOH,

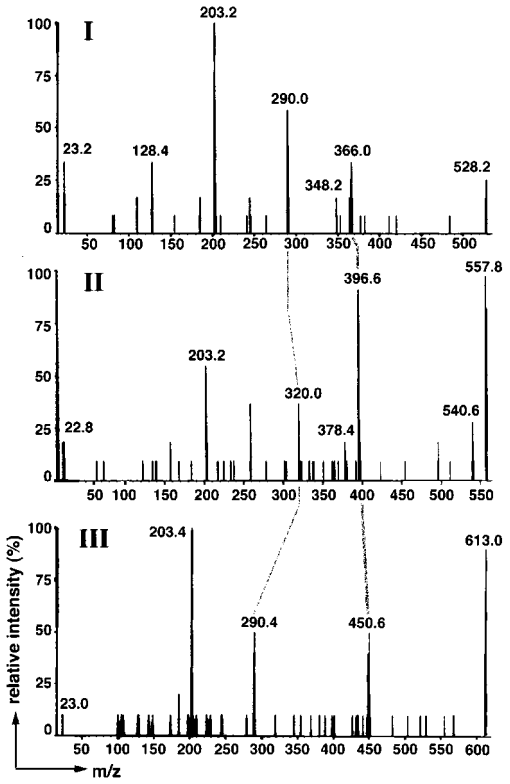

FIGURE 4: MS−MS spectra of serine and ceramide acids derived from GalC homologues: spectrum I, Gal^{P}C·^{S}COOH (M + Na); spectrum II, Gal^{P}C·^{C}COOH (M + Na); and spectrum III, Gal^{B}C·^{S}COOH (M + Na). MS analyses were performed on deprotected (by treatment with Et_3N/MeOH/H_2O) acids. For the lines drawn between spectra, thin lines correlate with ions formed from the loss of the acyl chain and thick lines with those from the loss of the glycal unit (see Scheme 5).

under neutral conditions could undergo cleavage between C4 and C5 to give the expected ceramide acid. In this case, the 4-oxo intermediate in the protected form would have been ^{3}CHOAc−^{4}CO−^{5}CHOH. It is possible that the treatment of ^{3}CHOAc−^{4}CO−^{5}CHOH with Et_3N/MeOH/H_2O (during deprotection) gave the rearranged product, i.e., the 3-oxo intermediate, ^{3}CO−^{4}CHOH−^{5}CHOH, along with the expected 4-oxo species, ^{3}CHOH−^{4}CO−^{5}CHOH.

Therefore, a similar rearrangement could have occurred during basic oxidation. We propose that the $KMnO_4$/$NaIO_4$ system gives the 4-oxo species ^{3}CHOAc−^{4}CO−^{5}CHOH (**B** in Scheme 4), as the intermediate, which under basic conditions (rapidly) rearranges to the 3-oxo species, ^{3}CO−^{4}CHOH−^{5}CHOH (**C** in Scheme 4), which in turn is cleaved to give the serine acids. We envisage intermediate **A**, where the participation of adjoining acetate function imposes specific steric and electronic constraints which, in turn, lead to the selective formation of **B**. The pH of the reaction medium could also influence the rate of periodate-mediated clevage of the 4-oxo species. Given that periodate-mediated diol oxidation is efficient under acidic conditions, the 4-oxo species formed under the basic conditions employed in the synthesis of serine acids is (kinetically) stable enough to undergo rearrangement to the 3-oxo intermediate.

MS analyses of the acetylated intermediate from neutral oxidation of (OAc)$_5$Gal^{S}C gave a molecular ion corresponding (probably) to intermediate **B** (^{3}CHOAc−^{4}CO−^{5}CHOH, 993.2, M + Na, 55%). A similar analysis of the intermediate

Scheme 5: Putative Fragmentation Analyses of the Sodium Adducts of Serine and Ceramide Acids[a]

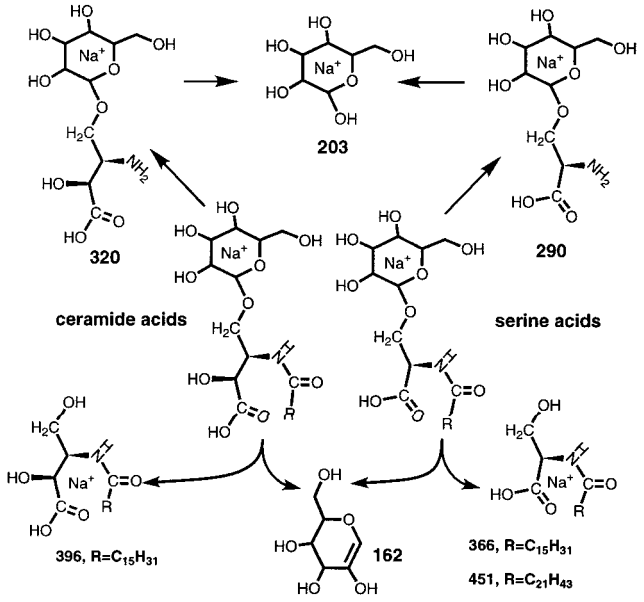

[a] The analyses were based on the acids derived from Gal^{B}C and Gal^{P}C homologues. The oxidized acids were deprotected with Et_3N/MeOH/H_2O and then analyzed by MS. Two types of fragmentation patterns, the loss of the acyl chain or the sugar (glycal unit), are correlated in Figure 3 with thin and broad lines, respectively. A similar pattern is also established in I−IV in Figure 4.

from basic oxidation gave **B** (22%) and **C** (^{3}CO−^{4}CHOH−^{5}CHOH, 951.0, M + Na, 14%) in an approximately 3:2 ratio. The finding of intermediate **C** in the sample from basic oxidation is consistent with the mechanism suggested in Scheme 4; however, the ratio of **B** was higher than that of **C**. It could be that under basic conditions, intermediate **C** is oxidized at a faster rate than **B**. MS−MS analyses of these peracetylated intermediates were limited due to the fragmentation of acetate units.

MS−MS Analysis of Serine and Ceramide Acids. Our objective in developing this microscale oxidation method was that it could be applied to GSLs isolated from tissue samples. Such samples (unless rigorously purified) contain "molecular debris", which complicates spectroscopic characterization (i.e., high chemical noise). For example, NMR analysis requires not only a larger quantity of sample but also a more pure sample. Particularly for natural GSLs, aglycone heterogeneity further complicates such spectroscopic analyses. In this respect, MS has the advantage, where the specific mass range of interest could be analyzed, and, techniques such as MS−MS can be used to evaluate structural information. Therefore, established patterns of CIDs for a class of molecules could be very useful. MS−MS analyses were carried out with serine and ceramide acids derived from GalC homologues, and their fragmentation patterns were analyzed.

The MS−MS spectra of the parent molecular ions, Gal^{P}C·^{C}COOH (558, M + Na), Gal^{P}C·^{S}COOH (528, M + Na), and Gal^{B}C·^{S}COOH (613, M + Na), are shown in Figure 4. All have peaks corresponding to the hexose fragment (203, hexose + Na) and Na ion (23, Na). Serine acids from palmitic and behenic analogues (I and III in Figure 4) exhibit a common ion at 290, suggesting the loss of acyl chains. This ion probably corresponds to the sodium adduct of serine galactoside (Scheme 5). A similar mode of fragmentation

Scheme 6: Putative Fragmentation Analysis of the Protonated Molecular Ions of Serine and Ceramide Acids[a]

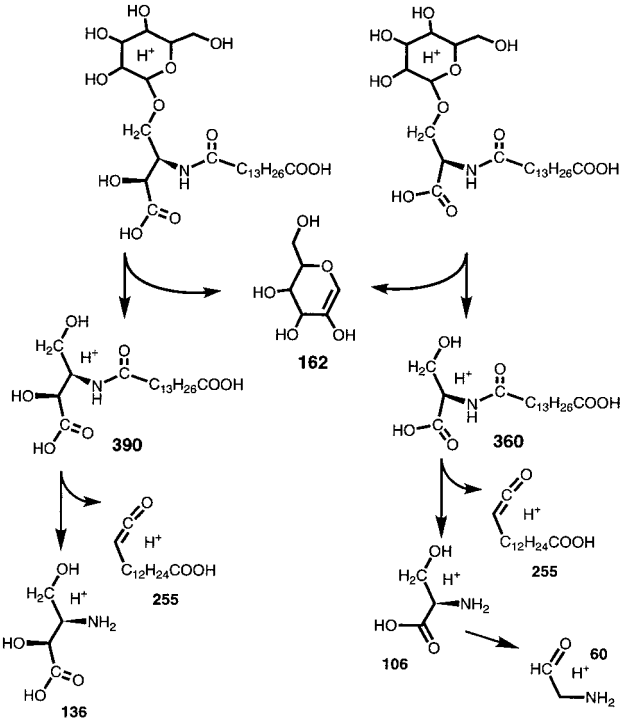

[a] Analyses were performed with samples derived from the oxidation of the nonhydroxylated fraction (type 1) of bovine GalC. The (basic and neutral) oxidized samples were treated with Et_3N/MeOH/H_2O and then analyzed by MS. The daughter ions resulting from the loss of glycal is correlated by a line in spectra V and VI in Figure 5.

for ceramide acid gave a fragment ion at 320 (**II** in Figure 4), with the expected mass difference of 30 mass units. The second preferred mode of CID involves the elimination of a glycal fragment (162, $C_6H_{10}O_5$), giving rise to the sodium adduct of only the oxidized ceramide portion (Scheme 5). This type of CID, for a given homologue, gave ions that differ by only 30 mass units. For example, Gal^{P}C·^{C}COOH and Gal^{P}C·^{S}COOH gave fragment ions at 396 and 366, respectively. However, ions from the same oxidation conditions, but with different acyl chains, will reflect some of the structural aspects (saturated, unsaturated, and hydroxylated) of the acyl chain. For example, Gal^{P}C·^{S}COOH and Gal^{B}C·^{S}COOH gave fragment ions at 366 and 450, respectively, and correspond to a difference of six CH_2 units. Other minor fragment ions result from the loss of water, or occasionally, serine acids exhibit additional loss of CO_2 (44 mass units) and/or formic acid (46 mass units).

Dicarboxylic acids, derived from GSLs containing unsaturated acyl chains, also follow fragmentation patterns similar to those discussed above. MS analyses of serine acids derived from Gal^{E}C and Gal^{O}C gave molecular ions consistent with GalC·^{S}COOH^{13}COOH (516, M + Na; and 538, M + 2Na) and GalC·^{S}COOH^{9}COOH (460, M + Na; and 482, M + 2Na), respectively. MS−MS analyses of these molecular ions showed the characteristic peak for serine acids at 290 (**I** and **II** in Figure 5). The fragment ions resulting from the loss of the glycal unit, 354 and 298, exhibited the expected mass difference of four CH_2 units.

To show an application of the established CIDs, MS−MS analyses were performed on the most abundant molecular ions of ceramide (III in Figure 5) and serine (IV in Figure

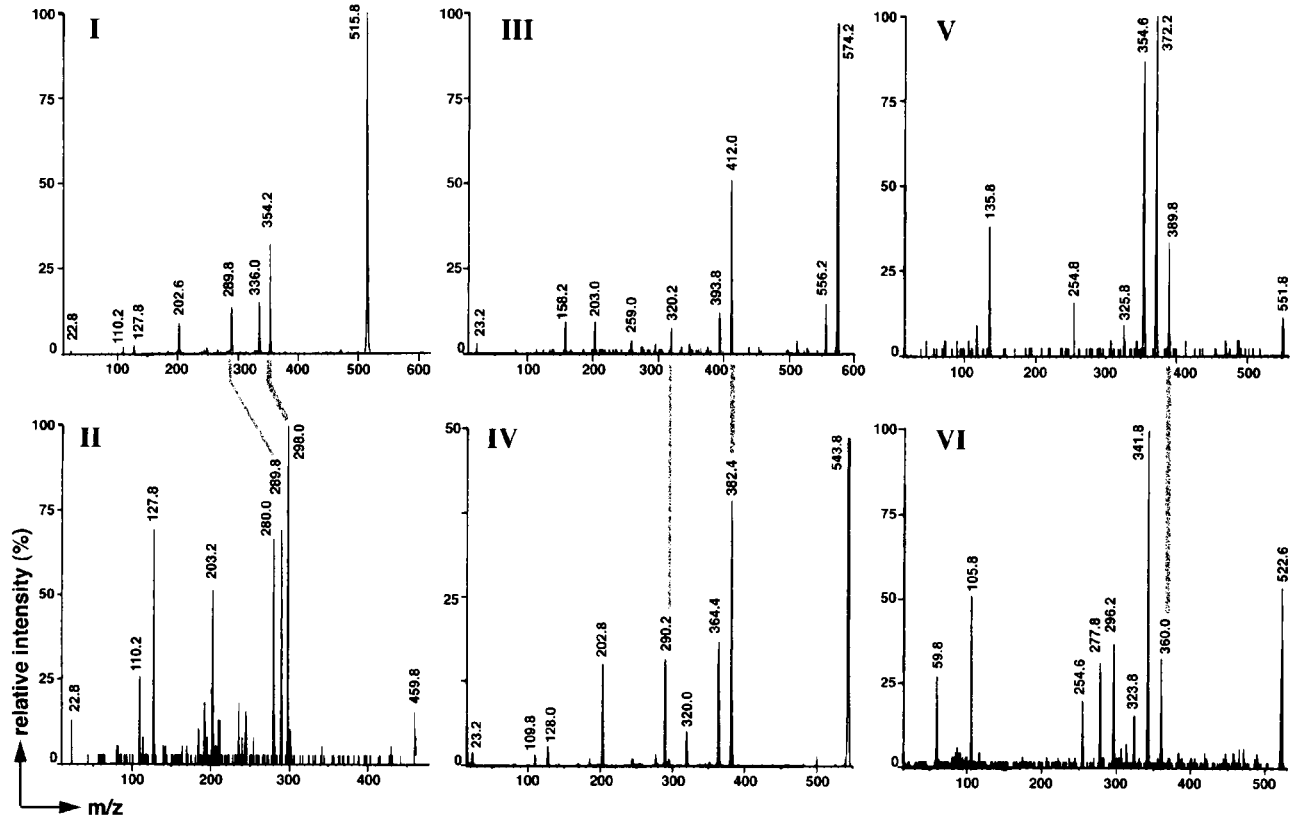

FIGURE 5: MS−MS spectra of serine and ceramide diacids derived from GalC homologues with unsaturated acyl chains and from natural bovine GalC: spectrum I, GalC·^{S}COOH^{13}COOH (M + Na), from Gal^{E}C; spectrum II, GalC·^{S}COOH^{9}COOH (M + Na), from Gal^{O}C; spectrum III, GalC·^{C}COOH^{15}COOH (M + Na); spectrum IV, GalC·^{S}COOH^{15}COOH (M + Na); spectrum V, GalC·^{C}COOH^{15}COOH (M + H); and spectrum VI, GalC·^{S}COOH^{15}COOH (M + H). Samples III−VI were from bovine (type 1) GalC. For the lines drawn between spectra, thin lines correlate with ions formed from the loss of the acyl chain and thick lines with those from the loss of the glycal unit (see Schemes 5 and 6).

5) acid samples synthesized from type I bovine GalC. Characteristic peaks for serine (at 290) and ceramide (at 320) acids were observed. Analyses of the ions resulting from the loss of the glycal fragment, 412 and 382, suggest that these daughter ions contain the acyl chain derived from a 15-carbon dicarboxylic acid. Therefore, we could determine that the parent ions, 574 and 544, correspond to GalC·^{C}COOH^{15}COOH and GalC·^{S}COOH^{15}COOH, respectively. The fragment ion at 320 (a rare coincidence) in spectrum IV of Figure 5 probably results from the loss of CO_2 (i.e., 364−44)

MS analyses also showed that serine and ceramide acids formed stable sodium adducts, M + Na (i.e., under the conditions employed), whereas protonated ions, M + H, were usually weak (<10%). MS−MS analyses of protonated molecular ions, from ceramide (V) and serine (IV) acids synthesized from type I bovine GalC, are shown in Figure 5. Interestingly, there were no peaks that would correspond to the characteristic ions, 290 and 320, observed during the CIDs of sodium adducts. All the CID patterns were centered on the ions resulting from the loss of the glycal unit, as shown in Scheme 6. The daughter ions, 390 (V in Figure 5) and 360 (VI in Figure 5), arise from the parent ions GalC·^{C}COOH^{15}COOH (552, M + H) and GalC·^{S}COOH^{15}COOH (522, M + H), respectively. These daughter ions undergo β-hydride elimination type CID of the acyl chain, where both granddaughter ions were observed. One such ion in the case of serine acids will be serine (106, M + H), and in the case of ceramide acids will be 2,4-dihydroxy-3-aminobutyric acid (136, M + H). Therefore, in the MS−MS analyses of M + H ions, peaks at 106 and 136 (which are comparable to the ions at 290 and 320 observed in the MS−MS analysis of M + Na ions) could be considered diagnostic of serine and ceramide acids, respectively. The second granddaughter ion, probably a protonated ketene (255, M + H), also provides information about the acyl chain (Scheme 6). Fragment ions from serine acids seem to lose a formic acid unit, likely from the serinecarboxylic acid. For example, ions at 60, 278, and 296 arise from 106, 324, and 342, respectively (VI in Figure 5). Also observed were ions resulting from the loss of water.

MS Profiles of Ceramide and Serine Acids from Natural GSLs. Negative ion MS profiles of ceramide (I) and serine (II) acids derived from bovine GalC (type I) are shown in Figure 6. Bovine GalC contains the unsaturated C-24:1 and the saturated C-24 acyl species at approximately 40 and 25%, respectively. However, the MS spectra of the oxidized products (in negative and positive ion modes) were dominated by the ions from the dicarboxylic acids, for example, GalC·^{C}COOH^{15}COOH. The acid containing the saturated acyl chain, Gal^{24}C·^{C}COOH, could only be observed in the negative ion mode, with a relative abundance of 3% (peaks at 646 in I and 616 in II). It seems that the negative ions (M − H) resulting from diacids were at least 20 times more stable than those from mono acids, and the stability of positive ions (M + Na) of diacids was even greater. However, for GSLs with mainly saturated acyl chains, the oxidized samples gave the corresponding ions in good

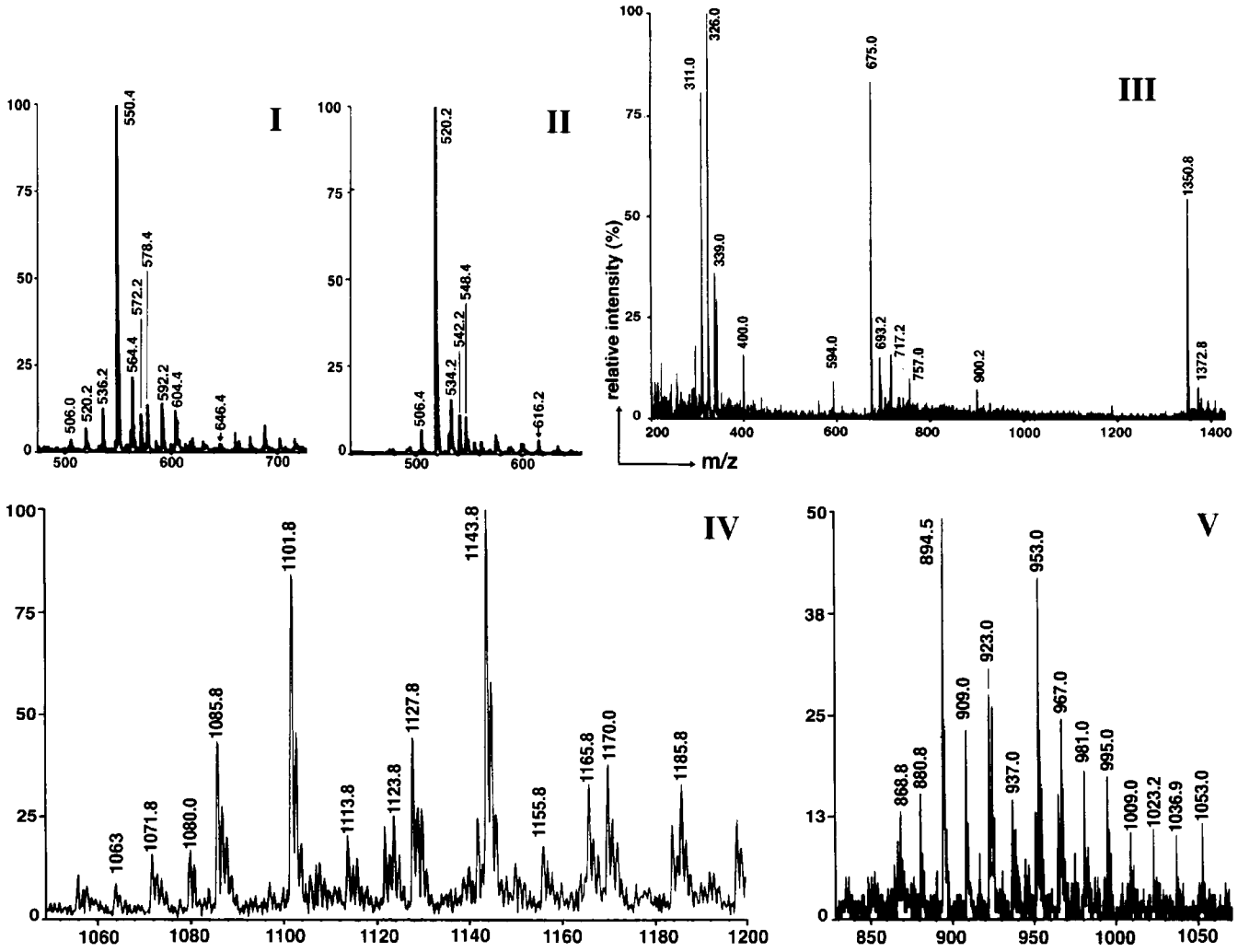

FIGURE 6: ESMS spectra of oxidized samples from natural GSLs: spectrum I, deprotected ceramide acids from bovine GalC (negative mode); spectrum II, deprotected serine acids from bovine GalC (negative mode); spectrum III, deprotected serine acids from bovine GM_1C (negative mode); spectrum IV, deprotected ceramide acids from HK-Gb_4C (positive mode); and spectrum V, peracetylated ceramide acids from bovine SGC (negative mode, showing *m/z* of singly charged ions). The results from samples IV and V are listed in Table 2.

abundance. For example, the serine acid derived from bovine GM_1C, which mainly contains $GM_1{}^{18}C$ (86%), gave molecular ions corresponding to singly charged (1350.8, M − H) and doubly charged (675.0, M − 2H) anions in approximately 55 and 80% relative abundance, respectively (III in Figure 6).

For higher-order GSLs (i.e., those with many sugars), the difference in the stability of ions derived from mono- and diacids seems to decrease. For example, Gb_4C from human kidney (HK) has a wide range of acyl chain heterogeneity. The MS spectrum of ceramide acids derived from HK-Gb_4C (IV in Figure 6) showed that ions from dicarboxylic acids were only 3 times more stable than those from monocarboxylic acids. Analyses of unoxidized HK-Gb_4C showed that the $Gb_4{}^{24}C$:$Gb_4{}^{24:1}C$ ratio was approximately 1:0.8, whereas the oxidized products $Gb_4{}^{C24}C$·$^{C}COOH$ and Gb_4C·$^{C}COOH^{C15}$-COOH appear in a 1:3 ratio (Table 2). Also seen in this particular MS spectrum are ions resulting from a monoacetate species (a trace impurity that results from incomplete deprotection) which gives very stable adducts with sodium, for example, 1143.8 [(OAc)Gb_4C·$^{C}COOHCOOH$ + Na, Table 2]. A similar situation was observed during the analysis of the $Gal^{B}C$·$^{C}COOH$, where (OAc)$Gal^{B}C$·$^{C}COOH$ gave a sodium adduct which was approximately 100 times more stable than the fully deprotected $Gal^{B}C$·$^{C}COOH$ (see Figures 1 and 2 and Table 1).

Dicarboxylic acids from charged GSLs (such as GM_1C or SGC) predominantly gave the doubly charged anions in the negative mode MS. For example, the higher mass range (800−1100) of the MS spectrum of the oxidized SGC showed two overlapping profiles of singly charge ions corresponding to hydroxylated (profile 1) and nonhydroxylated (profile 2) acyl chains (Figure 6 and Table 2). The expected M − H peak corresponding to diacid, $(OAc)_4SGC$·$^{C}COOH^{13}COOH$ (M − H, 771), was barely visible. However, the lower mass region of the spectrum consisted of a peak at *m/z* 385 (100%) which corresponds to the dianion of the diacid, $(OAc)_4SGC$·$^{C}COOH^{13}COOH$ (M − 2H, 385).

From the analyses presented above, it seems that a comparative MS study of the peracetylated GSL precursor and the oxidized (both neutral and basic conditions) material could provide a qualitative picture of the aglycone heterogeneity. This possibility was illustrated by the analyses of peracetylated GlcC from human Gaucher spleen and the (neutral) oxidized material. MS spectra are shown in Figure 7 and summarized in Table 3. Upon oxidation, GSLs with unsaturation in the aglycone are shifted to a different mass region in the MS spectra. Therefore, minor constituents such

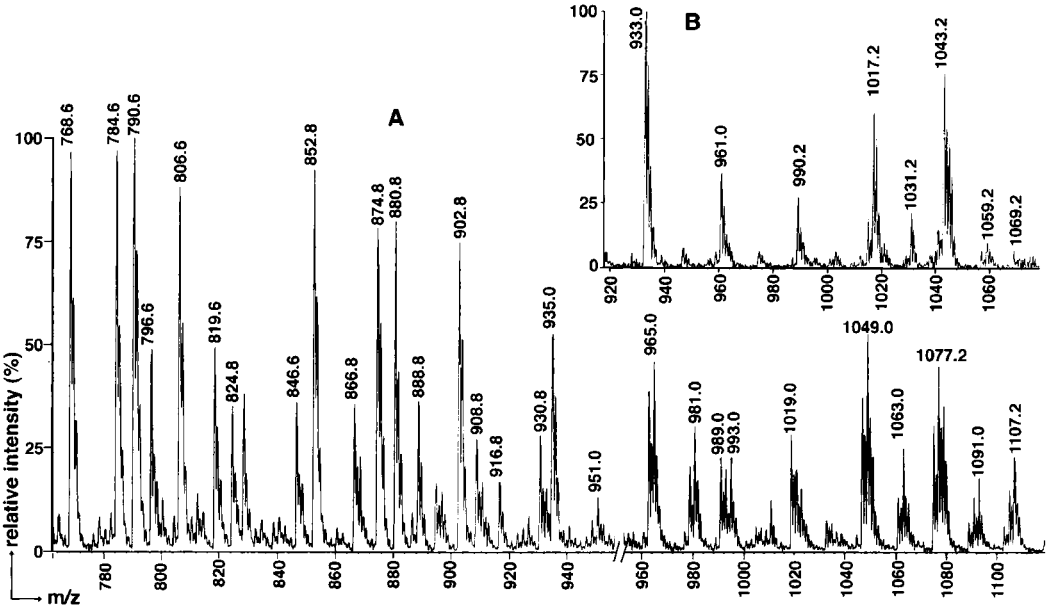

FIGURE 7: ESMS spectra of (neutral) oxidized GlcC (A) and the unoxidized GlcC (B). MS spectra were recorded with the peracetylated materials, and GlcC was from human Gauchers spleen. Results are listed in Table 3.

Table 2: Ions Observed in the Higher Mass Range of the ESMS Spectra of Ceramide Acids Derived from Gb_4C (deprotected sample, positive mode) and SGC (peracetylated sample, negative mode)[a]

acyl chain	Gb_4C[b] starting material M + Na (%)	Gb_4C oxidized ceramide mono- and diacids* M + H (%)	M + Na (%)	monoacetate M + Na (%)
16	1250.0 (25)	1063.0 (9)	1085.8 (44)	1127.8 (44)
18	1278.0 (5)		1113.8 (21)	1155.8 (18)
20	1306.0 (5)		1141.0(25)	
22	1334.0 (74)		1170.0 (38)	
24	1362.2 (100)		1198.0 (24)	
24:1	1360.0 (78)	1080.0* (17)	1101.8* (84)	1143.8* (100)

acyl chain (h = hydroxy)	starting material[b] SGC [M − H (%)]	SGC oxidized ceramide mono acids [M − H (%)]
22	1029.0 (10)	
h22	1087.0 (12)	923.0 (25)
23	1045.3 (12)	880.8 (14)
h23	1101.1 (5)	937.0 (15)
24	1059.4 (47)	894.8 (48)
24:1	1057.3 (100)	
h24	1117.2 (5)	953.0 (40)
h24:1	1115.4 (10)	
25	1073.0 (7)	909.0 (24)
h25		967.0 (26)
h26		981.0 (17)

[a] The species termed monoacetates is, for example, $(OAc)Gb_4{}^{16}C\cdot{}^{C}COOH$ (1127.8, M + Na), and arise from incomplete deprotection. A broader ESMS scan (200−1500) showed the following ions in the lower mass range. For Gb_4, ions corresponded to 730.4 (GalNAc-Gal-Gal-Glc + Na, 38%) and 356.2 $[(GalNAc\text{-}Gal\text{-}Gal\text{-}Glc + 2Na)^{2+}$, 100%]. For SGC, the dianion corresponding to the dicarboxylic acid at 385 $[(OAc)_4SGC\cdot{}^{C}COOH{}^{13}COOH$, 100%] was the most abundant peak. [b] Spectra not shown.

as dihydrosphingosine-containing GSLs (e.g., Glc^{16}*C) are now visible. Although most assignments are reasonable, a few, particularly the isobaric species, are ambiguous. Additional MS−MS analyses would help with further clarification. For example, MS−MS analyses of $Glc^{*16}C$ gave fragment ions that were consistent with a dihydrosphingosine-containing aglycone.

Neohydrocarbon Conjugates of Glycoserine and Ceramide Acids. We have recently demonstrated that ceramide acids derived from natural GSLs can be transformed into neoglycoproteins which could be used to study carbohydrate−protein interactions (*12*). Here we present the synthesis of novel neohydrocarbon glycoconjugates of glycosyl serine and ceramide acids and compare their receptor function. Specifically, the highly selective interaction between verotoxin and Gb_3C was investigated (*21*, *22*). Glycosyl serine and ceramide acids derived from natural bovine GalC, HK-LC, and HK-Gb_3C were coupled to rigid hydrocarbon "frames" such as adamantamine. Structurally, these neohydrocarbon conjugates will have one flexible acyl chain and a second rigid frame attached very close to the glycone, via the $^{C}COOH$ or the $^{S}COOH$ groups. Verotoxin binding profiles for these conjugates and their natural counterparts were investigated using TLC overlay and receptor ELISA binding (Figure 8). Both studies showed that verotoxin had a higher affinity for the neohydrocarbon conjugates than the corresponding natural GSLs. Adamantyl conjugates derived from LC (in the receptor ELISA assay) and GalC (by TLC overlay) exhibited no binding. These results show that the conjugates retain the specificity of the natural GSLs, except that their affinities were greatly enhanced.

The receptor ELISA results also show that the ceramide acid conjugate, $Gb_3C\cdot{}^{C}COHNAda$, bound VT in preference to the serine acid conjugate, $Gb_3C\cdot{}^{S}COHNAda$. As shown in Scheme 1, the ceramide acid conjugate (top left) has the additional hydroxy methylene unit. It is possible this hydroxy group could be involved in intra- and/or intermolecular hydrogen bonding. The crystal structure of cerebroside containing an α-hydroxy fatty acid reveals an intramolecular hydrogen bond involving the amide proton and the oxygen of the hydroxyl group of the fatty acid and the glycosidic oxygen (*23*). In the ceramide acid conjugates, the aglycone region consists of two amide linkages and one hydroxyl function, which could form intra- and/or intermolecular hydrogen bonds. Such hydrogen bonding could give rise to a degree of organization within the aglycone, which in turn

Table 3: MS Comparison of $GlcC(OAc)_5$ and the (Neutral) Oxidized Material $GlcC(OAc)_5{\cdot}^{C}COOH$[a]

aglycan	before oxidation	after oxidation	hydroxy acyl intermediate	ceramide monoacids M + Na, M − H + 2Na, etc.	ceramide diacids M + Na, M − H + 2Na	carboxy acyl M + Na, M − H + 2Na
$Glc^{16}C$	933.0 (100)		965.0 (45)	768.6 (96), 790.8 (100)		
$Glc^{18}C$	961.0 (37)		993.0 (21)	796.6 (50)		
$Glc^{20}C$	989 (28)		1021.0 (23)	824.8 (36), 846.6 (36) 868.8 (23)		
$Glc^{22}C$	1017.2 (66)[1]		1049.0 (53)[5]	852.8 (92), 874.8 (72)		
$Glc^{24}C$	1045 (<50)[2]		1077.0 (53)[6]	880.8 (81), 902.8 (75)		
$Glc^{22:1}$	1015.2 (20)		1047.0 (46)[3] 1079.0 (44) 1075.2 (34)[4]		C-15: 784.6 (98) 806.6 (89)	
$Glc^{24:1}C$	1043.2 (78)		1107.2 (33)			
$Glc^{16*}C$		935.0 (53)				
$Glc^{18*}C$		963.0 (39)				
$Glc^{20*}C$		991.0 (21)				
$Glc^{22*}C$		1019.0 (29)				
$Glc^{24*}C$		1047.2 (37)[3]				
$Glc^{26*}C$		1075.2 (37)[4]				
$Glc^{22:1*}C$	1017.2 (66)[1]		1049.0 (53)[5]			C-12: 908.8 (24) 930.8 (24)
$Glc^{24:1*}C$	1045.2 (50)[2]		1077.2 (53)[6]			

[a] Relative intensities are given in parentheses, and isobaric masses are indicated by superscript numbers. Ceramide monoacid, ceramide diacid, and carboxyacyl refer to $GlcC(OAc)_5{\cdot}^{C}COOH$, $GlcC(OAc)_5{\cdot}^{C}COOH^{n}COOH$, and $Glc^{*}C(OAc)_5{\cdot}^{n}COOH$, respectively.

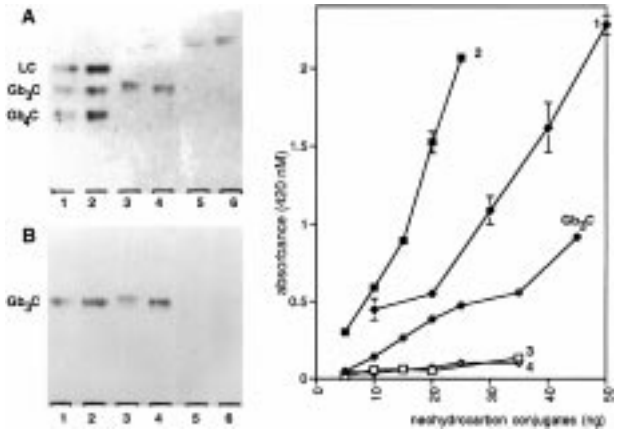

FIGURE 8: Verotoxin binding analyses of neohydrocarbon glycoconjugates. (Left panels) TLC overlay of compounds: 1, $Gb_3C{\cdot}^{S}COHNAda$; 2, $Gb_3C{\cdot}^{C}COHNAda$; 3, $LC{\cdot}^{S}COHNAda$; 4, $LC{\cdot}^{C}COHNAda$; 5, $GalC{\cdot}^{S}COHNAda$; and 6, $GalC{\cdot}^{C}COHNAda$. (A) Chemical staining with orcinol: lanes 1 and 2, 1 and 2 μg of natural neutral GSLs, respectively; lane 3, compound **1**; lane 4, compound **2**; lane 5, compound **5**; and lane 6, compound **6**. (B) Identical to plate A but VT binding visualized by the VT overlay assay. (Right panel) Receptor ELISA assay where glycoconjugates, as indicated, adsorbed to microtiter wells were probed for VT binding as described in Experimental Procedures.

could contribute to conformational and/or solvation factors that enhance the glycone−protein interactions. Moreover, the hydrocarbon frames, unlike planar aromatic rings, for example, are (probably) less likely to stack together. Insertion of such hydrophobic frames into the aglycone region of these neohydrocarbon aggregates (for example on the ELISA plate) is likely to enhance their flexibility and/or fluidity. This could be an additional contributing factor for achieving a favorable aglycone organization (discussed above).

When a natural GSL sample is transformed into a neohydrocarbon conjugate, as for example when coupled to adamantamine, there will be monoadamantyl ($GSL{\cdot}^{C}COAda$ or $GSL{\cdot}^{S}COAda$) and diadamantyl ($GSL{\cdot}^{C}COAda^{n}COAda$ or $GSL{\cdot}^{S}COAda^{n}COAda$) conjugates. Monoadamantyl species are derived from GSLs that contain saturated acyl chains, and the diadamantyl species is derived from those containing unsaturated acyl chains. The adamantyl groups that are attached to the $^{C}COOH$ or $^{S}COOH$ groups are closer to the glycone and probably play an important role in aglycone modulation.

Conclusions. Efficient and highly selective oxidation methods for the synthesis of 2-hydroxy-3-(*N*-acyl)-4-(*O*-glycosyl)oxybutyric acid (glycosyl ceramide acid) or 2-(*N*-acyl)-3-(*O*-glycosyl)oxypropionic acid (glycosyl serine acid) from natural GSLs have been developed. Mechanistic studies show the formation of an intriguing hydroxy−acyl intermediate. The products derived from dGSLs, the serine and ceramide oligosaccharides, can be used as precursors for the synthesis of neoglycoconjugates. Preliminary studies with neohydrocarbon glycoconjugates provide insight for designing unidentate, soluble GSL analogues. Also, the serine acids could be incorporated into specific amino acid sequences which may mimic certain glycoprotein motifs (*24*). The method provides a means of transforming a cellular GSL composition into the corresponding glycoconjugates, such as neohydrocarbon conjugates, reflecting cellular fatty acid heterogeneity. This would be difficult to achieve by purely synthetic methods. Furthermore, this oxidation can be used as an auxiliary method to characterize the aglycone heterogeneity of natural GSLs.

ACKNOWLEDGMENT

We thank the Toronto Carbohydrate Research Center (University of Toronto) for recording the mass spectra and B. Boyd and A. Nutikka for technical assistance.

REFERENCES

1. Hakomori, S. (1986) *Sci. Am. 254*, 40−53.
2. Hakomori, S. (1983) in *Sphingolipid Biochemistry* (Kanfer, J. N., and Hakomori, S., Eds.) Plenum Press, New York.
3. Stults, C. L. M., Sweeley, C. H., and Macher, B. A. (1989) *Methods Enzymol. 179*, 167−214.
4. Kiarash, A., Boyd, B., and Lingwood, C. A. (1994) *J. Biol. Chem. 269*, 11138−11146.
5. Sonnino, S., Kirschner, G., Ghidoni, R., Aquotti, D., and Tettamanti, G. (1985) *J. Lipid Res. 26*, 248−257.

6. Picking, W. D. (1993) *Biochem. Biophys. Res. Commun. 195*, 1153−1158.
7. Pagano, R., and Martin, O. (1988) *Biochemistry 27*, 4439−4445.
8. Young, W. W. J., Laine, R. A., and Hakomori, S. (1979) *J. Lipid Res. 20*, 275−278.
9. Laine, R., Yogeeswaren, G., and Hakomori, S. (1974) *J. Biol. Chem. 249*, 4460−4466.
10. MacDonald, D. L., Pat, L., and Hakomori, S. (1980) *J. Lipid Res. 21*, 642−645.
11. Seeberger, P. H., Bilodeau, M. T., and Danishefsky, S. J. (1997) *Aldrichim. Acta 30*, 75−92.
12. Mylvaganam, M., and Lingwood, C. A. (1999) *J. Biol. Chem. 274*, 20725−20732.
13. Lemieux, R. U., and von Rudloff, E. (1955) *Can. J. Chem. 33*, 1701−1709.
14. Boyd, B., Zhiuyan, Z., Magnusson, G., and Lingwood, C. A. (1994) *Eur. J. Biochem. 223*, 873−878.
15. Boyd, B., and Lingwood, C. A. (1989) *Nephron 51*, 207−210.
16. Head, S., Ramotar, K., and Lingwood, C. A. (1990) *Infect. Immun. 58*, 1532−1537.
17. Yamakawa, T., Irie, R., and Iwanaga, M. (1960) *J. Biochem. 48*, 490−497.
18. Boulanger, J., Petric, M., Lingwood, C. A., Law, H., Roscoe, M., and Karmali, M. (1990) *J. Clin. Microbiol. 28*, 2830−2833.
19. Lingwood, C. A., Law, H., Richardson, S., Petric, M., Brunton, J. L., DeGrandis, S., and Karmali, M. (1987) *J. Biol. Chem. 262*, 8834−8839.
20. Hsu, F.-F., Bohrer, A., and Turk, J. (1998) *Biochim. Biophys. Acta 1392*, 202−216.
21. Nyholm, P. G., Magnusson, G., Zheng, Z., Norel, R., Binnington-Boyd, B., and Lingwood, C. A. (1996) *Chem. Biol. 3*, 263−275.
22. Nyholm, P.-G., Brunton, J. L., and Lingwood, C. A. (1995) *Int. J. Biol. Macromol. 17*, 199−205.
23. Pascher, I., and Sundell, S. (1977) *Chem. Phys. Lipids 20*, 175−191.
24. Kuduk, S. D., Schwarz, J. B., Chen, X. T., Glunz, P. W., Sames, D., Ragupathi, G., Livingston, P. O., and Danishefsky, S. J. (1998) *J. Am. Chem. Soc. 120*, 12474−12485.

BI990669M